

# Turbulent diffusion with rotation or magnetic fields

Axel Brandenburg,<sup>1</sup>\* Andreas Svedin<sup>2</sup> and Geoffrey M. Vasil<sup>3</sup>

<sup>1</sup>*NORDITA, AlbaNova University Center, Roslagstullsbacken 23, SE - 106 91 Stockholm, Sweden*

<sup>2</sup>*Astronomy Department, Columbia University, New York 10027, USA*

<sup>3</sup>*JILA, University of Colorado, Boulder, CO 80309-0440, USA*

Accepted 2009 February 16. Received 2009 February 16; in original form 2009 January 15

## ABSTRACT

The turbulent diffusion tensor describing the evolution of the mean concentration of a passive scalar is investigated for non-helically forced turbulence in the presence of rotation or a magnetic field. With rotation, the Coriolis force causes a sideways deflection of the flux of mean concentration. Within the magnetohydrodynamics approximation there is no analogous effect from the magnetic field because the effects on the flow do not depend on the sign of the field. Both rotation and magnetic fields tend to suppress turbulent transport, but this suppression is weaker in the direction along the magnetic field. Turbulent transport along the rotation axis is not strongly affected by rotation, except on shorter length-scales, i.e. when the scale of the variation of the mean field becomes comparable with the scale of the energy-carrying eddies. These results are discussed in the context of anisotropic convective energy transport in the Sun.

**Key words:** hydrodynamics – magnetic fields – MHD – turbulence.

## 1 INTRODUCTION

In the outer 30 per cent of the Sun, energy is transported mainly by convection through the exchange of fluid parcels. This process tends to smear out entropy gradients by making the gas nearly isentropic on the average. Any remaining entropy gradients lead to a mean entropy flux whose negative divergence leads to a local change in the entropy. This entropy flux is equal to the negative gradient of the mean entropy multiplied by some turbulent diffusivity coefficient. Using mixing length theory, this turbulent diffusion coefficient is found to be of the order of the turbulent velocity times some mixing length, which is often taken as a free parameter (Vitense 1953).

With rotation, the smearing out of entropy gradients is significantly reduced due to lateral mixing generated by Coriolis deflections (Julien et al. 1996). Such deflections cause fluid parcels to lose their heat content to the sides before they can ascend or descend and transport heat vertically. This additional mixing explains why the smearing out of entropy gradients is heavily reduced by rotation. Rotational effects on the turbulent diffusivity were already studied by Weiss (1965) and Durney & Roxburgh (1971) who found that the turbulent diffusion tensor becomes anisotropic with respect to the direction of the rotation axis. The components of the anisotropic diffusion tensor can be computed using the first-order smoothing approximation (Rüdiger 1989; Kitchatinov, Rüdiger & Pipin 1994). These calculations show that the enhancement of turbulent diffusion along the direction of rotation corresponds to a latitudinal heat

flux towards the pole, making it slightly hotter. Turbulent convection simulations by Rüdiger et al. (2005) confirm this, but they also show that the radial heat flux is slightly smaller near the poles, which is explained by the effect of stratificational anisotropy. This agrees with earlier results of Rieutord et al. (1994) and Käpylä, Korpi & Tuominen (2004). Rüdiger et al. (2005) also established the presence of an azimuthal turbulent heat flux and found it to be negative, that is in the westward direction. This was surprising in view of the result of Kitchatinov et al. (1994) who found it to be either zero (for a simple mixing length model) or positive (for a turbulence model with finite-time correlation effects). However, their result was based on a sign error (Rüdiger, private communication). Furthermore, if there is also stratification, the simple mixing length model of Kitchatinov et al. (1994) predicts that the sign of the flux should agree with that of the corresponding component of the Reynolds stress tensor and hence negative, which is then in agreement with the convection simulations of Rüdiger et al. (2005).

Diffusive processes also play a role in the evolution of the mean magnetic field and the mean momentum. In recent years, it has become possible to compute the relevant diffusion coefficients together with other (e.g. non-diffusive) turbulent transport coefficients using turbulence simulations. In the case of magnetic fields, a fairly accurate method is the test field method in which one solves an additional set of passive evolution equations for the departures from the corresponding set of prescribed mean fields (Brandenburg 2005; Schrunner et al. 2005, 2007; Brandenburg et al. 2008a).

In cases of poor scale separation, i.e. when the scale of the mean field is only a few times larger than the typical scale of the turbulence, the multiplication with a diffusion coefficient must be

\*E-mail: brandenb@nordita.org

replaced by a convolution with an integral kernel. A similar situation also applies to cases where the time-scale of the variation of the mean fields becomes comparable with the turnover time. In such cases, the test field method has also been used to determine the integral kernels (Brandenburg et al. 2008a; Hubbard & Brandenburg 2008). If the turbulence is anisotropic and/or inhomogeneous, the diffusion coefficients or kernels are replaced by tensors. Again, the test field method allows an accurate determination of all relevant tensor components.

In this paper, we apply the test field method to the turbulent diffusion of entropy in cases where the turbulence is homogeneous, but anisotropic due to the presence of rotation or a magnetic field. The former problem has recently been addressed by Rüdiger et al. (2005), who evaluated the actual fluxes in stratified turbulent convection. However, convection necessarily imposes an additional anisotropy in the direction of gravity, so it becomes harder to disentangle the effects of gravity and rotation. Here, we focus on the case of forced turbulence in the absence of gravity; using an isothermal equation of state. In that case, the evolution equation of entropy is similar to that of a passive scalar.

The effect of rotation on turbulent diffusion is important for modelling the possibility of latitudinal entropy gradients in rotating stars, that is, perpendicular to the radial direction of the energy flux. Latitudinal entropy gradients could be important for producing a significant baroclinic term that would balance the curl of the Coriolis force and could therefore be important for explaining the observation that the contours of constant angular velocity in the Sun are not parallel to the rotation axis (Kitchatinov & Rüdiger 1995; Thompson et al. 2003). The effect of a magnetic field on turbulent heat diffusion is important in the theory of sunspots (e.g. Kitchatinov & Mazur 2000) where the energy transport is suppressed in an anisotropic fashion (Rüdiger & Hollerbach 2004). Furthermore, anisotropic passive scalar transport is important in connection with understanding the partial lithium depletion in the Sun (Rüdiger & Pipin 2001).

## 2 PRELIMINARY CONSIDERATIONS

We make use of the fact that in the absence of gravity, and with an isothermal equation of state the evolution of entropy is passive, i.e. there is no feedback on the momentum equation. We can therefore consider the evolution equation for a passive scalar concentration per unit volume  $C$ , which obeys

$$\frac{\partial C}{\partial t} = -\nabla \cdot (UC) + \kappa \nabla^2 C, \quad (1)$$

where  $\kappa$  is the diffusivity and  $\mathbf{U}$  is the velocity. We note that in the compressible case there is an extra term  $-\kappa \nabla \cdot (C \nabla \ln \rho)$  on the right-hand side of equation (1) where  $\rho$  is the density.

The evolution of the mean concentration  $\bar{C}$  is obtained by averaging equation (1), which yields

$$\frac{\partial \bar{C}}{\partial t} = -\nabla \cdot (\bar{\mathbf{U}} \bar{C} + \overline{\mathbf{u}C}) + \kappa \nabla^2 \bar{C}, \quad (2)$$

where  $\overline{\mathbf{u}C} \equiv \bar{\mathcal{F}}$  is the mean flux of the concentration density. Under the assumption that the spatial and temporal scales of the mean field are well separated from those of the turbulence, one can make a generalized Fickian diffusion ansatz of the form:

$$\bar{\mathcal{F}}_i = -\kappa_{ij} \nabla_j \bar{C}, \quad (3)$$

where  $\kappa_{ij}$  is the turbulent diffusion tensor. In the absence of good scale separation, the multiplication with a diffusion tensor must be

replaced by a convolution with an integral kernel. We discuss this case near the end of the paper, but ignore this for now.

The turbulent diffusion tensor is a proper tensor, so in the presence of rotation and in the absence of helicity it has only even powers of the pseudo vector  $\boldsymbol{\Omega}$  and odd powers of  $\boldsymbol{\Omega}$  combined with odd powers of the Levi–Civita tensor. It must therefore have the general form (Kitchatinov et al. 1994),

$$\kappa_{ij} = \kappa_t \delta_{ij} + \kappa_\Omega \epsilon_{ijk} \hat{\Omega}_k + \kappa_{\Omega\Omega} \hat{\Omega}_i \hat{\Omega}_j, \quad (4)$$

where  $\hat{\boldsymbol{\Omega}} = \boldsymbol{\Omega}/|\boldsymbol{\Omega}|$  is the unit vector along the rotation axis and  $\kappa_t$ ,  $\kappa_\Omega$  and  $\kappa_{\Omega\Omega}$  are functions of the Coriolis, Peclet and Schmidt numbers, that are defined by

$$\text{Co} = \frac{2\Omega}{u_{\text{rms}} k_f}, \quad \text{Pe} = \frac{u_{\text{rms}}}{\kappa k_f}, \quad \text{and} \quad \text{Sc} = \frac{\nu}{\kappa}, \quad (5)$$

respectively. Incidentally, we note that  $\kappa_\Omega$  contributes an anti-symmetric component to the turbulent diffusion tensor, which does not contribute to divergence of flux. Similarly, in the presence of a magnetic field  $\mathbf{B}$  with unit vector  $\hat{\mathbf{B}} = \mathbf{B}/|\mathbf{B}|$ , the diffusion tensor must have the form

$$\kappa_{ij} = \kappa_t \delta_{ij} + \kappa_B \epsilon_{ijk} \hat{B}_k + \kappa_{BB} \hat{B}_i \hat{B}_j, \quad (6)$$

but here  $\kappa_B = 0$  because the diffusion tensor can only depend on the Lorentz force which is quadratic in  $\mathbf{B}$ , so  $\kappa_{ij}$  must be invariant under a change of sign of  $\mathbf{B}$  (Kitchatinov et al. 1994). Thus, we have only  $\kappa_t$  and  $\kappa_{BB}$  that are functions of  $|\mathbf{B}|/B_{\text{eq}}$ , Pe and Sc, where

$$B_{\text{eq}} = \langle \mu_0 \rho \mathbf{U}^2 \rangle^{1/2} \quad (7)$$

is the equipartition field strength, and  $\mu_0$  is the vacuum permeability.

By adding rotation or by imposing a magnetic field, the flow becomes anisotropic. The degree of anisotropy is characterized by the parameter

$$\varepsilon = 1 - \frac{\overline{u_\perp^2}}{\overline{u_\parallel^2}}, \quad (8)$$

where  $\overline{u_\perp^2}$  and  $\overline{u_\parallel^2}$  are the velocity dispersions perpendicular and parallel to the direction of anisotropy,  $\hat{\boldsymbol{\Omega}}$  or  $\hat{\mathbf{B}}$ . In practice, we take these directions to be the  $z$  direction, in which case  $\overline{u_\parallel^2} = \overline{u_z^2}$  and  $\overline{u_\perp^2}$  is calculated as  $(1/2)(\overline{u_x^2} + \overline{u_y^2})$ . Isotropy implies  $\varepsilon = 0$ .

## 3 METHOD

We simulate turbulence by solving the compressible hydromagnetic equations with an imposed random forcing term and an isothermal equation of state, so that the pressure  $p$  is related to  $\rho$  via  $p = \rho c_s^2$ , where  $c_s$  is the isothermal sound speed. We consider a periodic Cartesian domain of size  $L^3$ . In the presence of an imposed field  $\mathbf{B}_0$ , we write the total field as  $\mathbf{B} = \mathbf{B}_0 + \nabla \times \mathbf{A}$ , where  $\mathbf{A}$  is the magnetic vector potential. In the non-magnetic case, we put  $\mathbf{B}_0 = \mathbf{0}$ , and with  $\mathbf{A} = \mathbf{0}$  initially, we have  $\mathbf{B} = \mathbf{0}$  for all times, and the hydromagnetic equations reduce to the Navier–Stokes equations for  $\rho$  and  $\mathbf{U}$ ,

$$\frac{D \ln \rho}{Dt} = -\nabla \cdot \mathbf{U}, \quad (9)$$

$$\frac{D\mathbf{U}}{Dt} = -2\boldsymbol{\Omega} \times \mathbf{U} - c_s^2 \nabla \ln \rho + \mathbf{f} + \mathbf{F}_{\text{visc}} + \mathbf{F}_{\text{Lor}}, \quad (10)$$

where  $\mathbf{F}_{\text{Lor}} = \mathbf{0}$  in the non-magnetic case, i.e. there is no Lorentz force,  $D/Dt = \partial/\partial t + \mathbf{U} \cdot \nabla$  is the advective derivative,  $\boldsymbol{\Omega}$  is the background angular velocity,  $\mathbf{F}_{\text{visc}} = \rho^{-1} \nabla \cdot 2\rho\nu\mathbf{S}$  is the viscous force,  $\nu$  is the kinematic viscosity,  $\mathbf{S}_{ij} = (1/2)(U_{i,j} + U_{j,i}) - (1/3)\delta_{ij} \nabla \cdot \mathbf{U}$  is the traceless rate of strain tensor, and  $\mathbf{f}$  is a random

forcing function consisting of plane transversal waves with random wavevectors  $\mathbf{k}$  such that  $|\mathbf{k}|$  lies in a band around a given forcing wavenumber  $k_f$ . The vector  $\mathbf{k}$  changes randomly from one time-step to the next. This method is described for example in Haugen, Brandenburg & Dobler (2004). The forcing amplitude is chosen such that the Mach number  $\text{Ma} = u_{\text{rms}}/c_s$  is about 0.1.

In the magnetic case, we have a finite Lorentz force  $\mathbf{F}_{\text{Lor}} = \mathbf{J} \times \mathbf{B}/\rho$ , where  $\mathbf{J} = \nabla \times \mathbf{B}/\mu_0$  is the current density,  $\mu_0$  is the vacuum permeability, and we solve the uncurled induction equation in the form

$$\frac{\partial \mathbf{A}}{\partial t} = \mathbf{U} \times \mathbf{B} + \eta \nabla^2 \mathbf{A}, \quad (11)$$

where  $\eta$  is the magnetic diffusivity, which is assumed constant.

The test scalar equation is obtained by subtracting equation (2) from equation (1), which yields

$$\frac{\partial c}{\partial t} = -\nabla \cdot (\overline{\mathbf{U}}c + \mathbf{u}\overline{c} + \mathbf{u}c - \overline{\mathbf{u}c}) + \kappa \nabla^2 c, \quad (12)$$

where  $c = C - \overline{C}$  and  $\mathbf{u} = \mathbf{U} - \overline{\mathbf{U}}$  are the fluctuating values of concentration and velocity and  $\overline{\mathbf{u}c}$  is the mean flux of concentration density. We restrict ourselves to the case of two-dimensional mean fields,  $\overline{C} = \overline{C}(x, z, t)$ , that are obtained by averaging over the  $y$  direction. In the spirit of the test field method, we solve equation (1) for a pre-determined set of four different mean fields,

$$\overline{C}^{c0} = C_0 \cos kx, \quad \overline{C}^{s0} = C_0 \sin kx, \quad (13)$$

$$\overline{C}^{0c} = C_0 \cos kz, \quad \overline{C}^{0s} = C_0 \sin kz, \quad (14)$$

where  $C_0$  is a normalization factor, that will drop out in the determination of  $\kappa_{ij}$  since equation (3) is linear. For each of these mean fields  $\overline{C}^{pq}$ , we obtain a separate evolution equation for  $c^{pq}$ ,

$$\frac{\partial c^{pq}}{\partial t} = -\nabla \cdot (\overline{\mathbf{U}}c^{pq} + \mathbf{u}\overline{C}^{pq} + \mathbf{u}c^{pq} - \overline{\mathbf{u}c^{pq}}) + \kappa \nabla^2 c^{pq}, \quad (15)$$

where  $p, q = c, s$  or  $0$ . In this way, we calculate four different fluxes,  $\overline{\mathcal{F}}^{pq} = \overline{\mathbf{u}c^{pq}}$ , and compute the six relevant components of  $\kappa_{ij}$ ,

$$\kappa_{i1} = -\langle \cos kx \overline{\mathcal{F}}_i^{s0} - \sin kx \overline{\mathcal{F}}_i^{c0} \rangle / k, \quad (16)$$

$$\kappa_{i3} = -\langle \cos kz \overline{\mathcal{F}}_i^{0s} - \sin kz \overline{\mathcal{F}}_i^{0c} \rangle / k, \quad (17)$$

for  $i = 1, \dots, 3$ . Here, angular brackets denote volume averages. The expressions for  $\kappa_{i1}$  and  $\kappa_{i3}$  in equations (16) and (17) differ in that the superscripts  $s0$  and  $c0$  are replaced by  $0s$  and  $0c$ , respectively. Note that the components of  $\kappa_{ij}$  for  $j = 2$  are irrelevant for mean fields that are independent of  $y$ .

The method provides the functions  $\kappa_t$ ,  $\kappa_\Omega$  and  $\kappa_{\Omega\Omega}$  (or  $\kappa_B$  and  $\kappa_{BB}$ ) as functions of  $z$  and  $t$ . Unless otherwise specified, we quote averages over  $z$  and  $t$ . Error bars are calculated by averaging the results first over  $z$  and then over subsequent time intervals  $\Delta t$  whose length corresponds to one correlation time, that is  $\Delta t u_{\text{rms}} k_f = 1$ . This results in a number of independent measurements from which we calculate the standard deviation, which is what we quote as the error.

The simulations have been carried out using the `PENCIL` code<sup>1</sup> which is a high-order finite-difference code (sixth order in space and third order in time) for solving the compressible hydro-magnetic equations. As of revision `r10245`, the test scalar equations are implemented into the public-domain code similar to

the way described above and are invoked by compiling with `TESTSCALAR=testsclar`.<sup>2</sup> The numerical resolution used in the simulations depends on the Peclet number and reaches  $256^3$  mesh-points for our runs with  $\text{Pe} \approx 200$ .

## 4 RESULTS

As in earlier work on determining the turbulent magnetic diffusivity using the test field method, we present our results for the relevant components of  $\kappa_{ij}$  by normalizing them with respect to the reference value

$$\kappa_{10} = \frac{1}{3} u_{\text{rms}} k_f^{-1}. \quad (18)$$

This is motivated by the first order smoothing result  $\kappa_t = \frac{1}{3} \tau u_{\text{rms}}^2$  and the assumption that the Strouhal number  $\text{St} = \tau u_{\text{rms}} k_f$  is about unity (Brandenburg et al. 2004). We focus on the case  $k_f/k_1 \approx 3$ , which is a compromise of having enough wavenumbers between  $k_f$  and the dissipation wavenumber (which is where an inertial range can develop), and leaving some room for scales larger than that of the energy-carrying eddies corresponding to wavenumber  $k_f$ . On a few occasions, we also consider other values of  $k_f/k_1$ .

We begin by considering the case with rotation and no magnetic field. In Fig. 1, we compare the dependence of  $\kappa_t$ ,  $\kappa_\Omega$ , and  $\kappa_{\Omega\Omega}$  on  $\text{Co}$  for fixed values of  $\text{Pe} = 1.8$  and  $120$ , using  $\text{Sc} = 1$  in all cases. Note that  $\kappa_t$  shows a mild decline with  $\text{Co}$  while both  $\kappa_\Omega$  and  $\kappa_{\Omega\Omega}$  are positive and increase with  $\text{Co}$ . For  $\text{Pe} = 1.8$ , the results can be fitted to expressions of the form  $\kappa_t \approx 0.7/[1 + (0.3 \text{Co})^2]$ ,  $\kappa_\Omega \approx 0.25 \text{Co}/[1 + (0.5 \text{Co})^2]$ , and  $\kappa_{\Omega\Omega} \approx 0.05 \text{Co}/[1 + (0.05 \text{Co})^2]$ . For larger values of  $\text{Pe}$ , the dependence of  $\kappa_t$  and  $\kappa_\Omega$  on  $\text{Co}$  is qualitatively similar, but the dependence of  $\kappa_{\Omega\Omega}$  on  $\text{Co}$  now shows indications of a sign change for larger values of  $\text{Co}$ . A positive  $\kappa_\Omega$  would agree with the result of Rüdiger et al. (2005), although their result was explained to be due to the additional effect of stratification.

The dependence of  $\kappa_t$ ,  $\kappa_\Omega$  and  $\kappa_{\Omega\Omega}$  on  $\text{Pe}$  for  $\text{Co} = 0.5$  and  $\text{Sc} = 1$  is shown in Fig. 2. As expected, for very small values of  $\text{Pe}$ , all three functions go to zero like  $\kappa_t/\kappa_{10} \approx 0.4 \text{Pe}$  and  $\kappa_\Omega/\kappa_{10} \approx 0.05 \text{Pe}^2$ , while  $\kappa_{\Omega\Omega}$  is close to zero and, within error bars, essentially compatible with zero. For large values of  $\text{Pe}$ , both  $\kappa_t$  and  $\kappa_\Omega$  seem to reach asymptotic values, while for  $\kappa_{\Omega\Omega}$  there is no clear trend. An asymptotic value of  $\kappa_t$  was expected based on the analogy with the magnetic case where the magnetic diffusivity was also found to reach an asymptotic value for large Reynolds numbers (Sur, Brandenburg & Subramanian 2008).

In all our cases, we find that  $\kappa_\Omega$  is positive. This result is in agreement with that of Rüdiger et al. (2005), who define a quantity  $\tilde{\chi}$  such that  $\tilde{\chi}\Omega = -\kappa_\Omega$ . They point out that in spherical coordinates  $(r, \theta, \phi)$  a finite  $\kappa_\Omega$  corresponds to a finite  $\kappa_{r\phi}$  which, in turn, leads to a finite azimuthal heat flux. Its astrophysical importance is limited because the azimuthal average of its divergence vanishes. However, Rüdiger et al. (2005) stress that the sign and magnitude of  $\kappa_\Omega$  provides an important test of mean-field theory. Their result was motivated using a result from the mixing-length model of Kitchatinov et al. (1994) that  $\kappa_{ij}$  should be proportional to the Reynolds-stress tensor  $\overline{u_i u_j}$ . A positive  $\kappa_\Omega$  would correspond to a negative  $\kappa_{r\phi}$ , which could be explained by a negative  $\overline{u_r u_\phi}$  that is expected for stratified turbulence with dominant vertical turbulent velocities. This argument, which is originally due to Gough (1978), does not apply in our case. However, a positive value of  $\kappa_\Omega$  is an

<sup>1</sup> <http://www.nordita.org/software/pencil-code>

<sup>2</sup> <http://pencil-code.googlecode.com/>

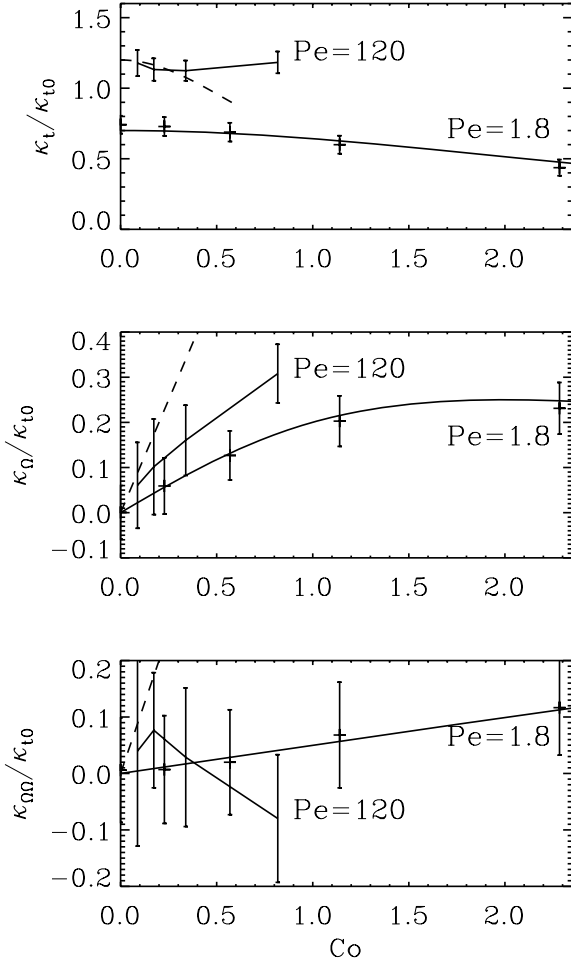


**Figure 1.** Co dependence of  $\kappa_t$ ,  $\kappa_\Omega$  and  $\kappa_{\Omega\Omega}$  for  $Pe = 1.8$  and  $120$ . For  $Pe = 1.8$ , the results can be fitted to expressions described in the text, while for larger values of  $Pe$  the dependences tend to be more complicated. The dashed lines indicate the behaviour expected from the simple treatment of the  $\tau$  approximation in Appendix A. The slope of the dashed lines in the middle and last panel is therefore 1. For these runs, the anisotropy parameter  $\varepsilon$  varies between 0 and 0.04.

immediate consequence of the Coriolis force producing systematic sideways motions; see Fig. 3. That is, suppose there exists a mean concentration gradient in, say, the positive  $x$ -direction, that is  $\nabla\bar{C} \sim \hat{x}$ . Then a small fluid parcel that is moving in the down-gradient direction,  $\mathbf{u} \sim -\nabla\bar{C}$ , would experience, via the Coriolis acceleration, a deflection into the positive  $y$ -direction. The mean effect of such deflections would be to produce a positive coherent flux in the direction given by  $-\nabla\bar{C} \times \hat{\Omega}$ , and thus  $\kappa_\Omega$  must be positive. A positive value of  $\kappa_\Omega$  can also be explained using the pressureless  $\tau$  approximation which predicts  $\kappa_\Omega/\kappa_t = Co$ ; see Appendix A. This underlines the potential usefulness of the  $\tau$  approximation in mean-field theory, even if this approach is used in its most rudimentary form.

The simple treatment of the  $\tau$  approximation in Appendix A predicts that  $\kappa_t$  declines with increasing values of  $Co$ , while both  $\kappa_\Omega$  and  $\kappa_{\Omega\Omega}$  increase and are positive. This is in agreement with the simulations, but quantitative details are not reproduced: in the simulations the decline of  $\kappa_t$  as well as the increase of  $\kappa_\Omega$  and  $\kappa_{\Omega\Omega}$  are slower than what is predicted by the simple treatment of the  $\tau$  approximation. There could be several reasons for this departure of the simulations from theory. First, the definition of  $Co$  is not

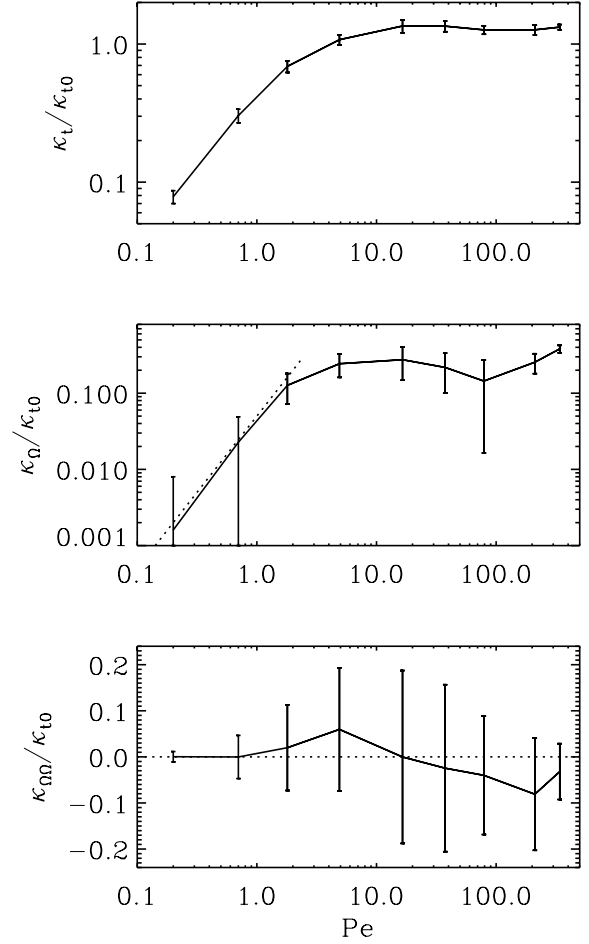


**Figure 2.** Pe dependence for  $Co = 0.5$  keeping  $Sc = 1$  in all cases. The resolution is increased with increasing values of  $Pe$  and reaches  $256^3$  for the run with the largest value of  $Pe$ .

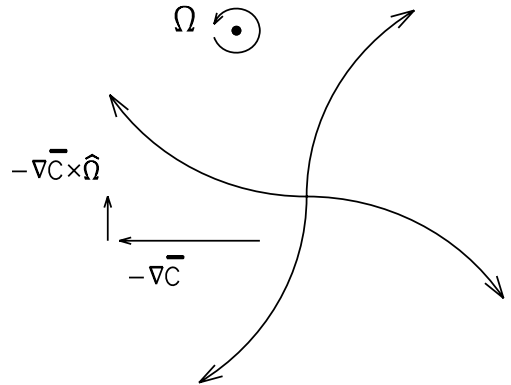


**Figure 3.** Sketch illustrating the systematic sideways motion caused by the Coriolis force and its effect on the flux and hence the sign of  $\kappa_\Omega$ .

unique. However, even for small values of  $Pe$  the functions  $\kappa_t$ ,  $\kappa_\Omega$  and  $\kappa_{\Omega\Omega}$  would require different scaling factors on  $Co$  to fit the results (see above). Secondly, the feedback of rotational effects on the Reynolds stresses are not taken into account in the simple form of the  $\tau$  approximation. On the other hand, the rotational anisotropy parameter  $\varepsilon$  remains fairly small (below 0.04) even for the largest values of  $Co$  considered. The correlation  $\overline{f^c}$  was neglected, but this should be permissible in the current case with  $\delta$ -correlated forcing;

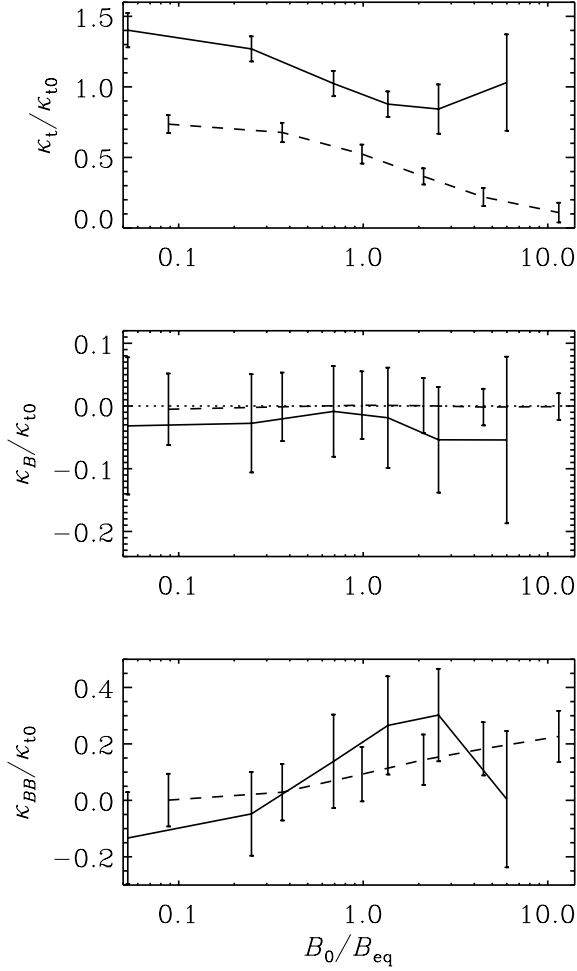


**Figure 4.** Dependence on the magnetic field strength for  $Pe = 1.8$  (dashed) and for  $Pe$  in the range 12–15 (solid). For these runs, the anisotropy parameter  $\varepsilon$  varies between 0 and 0.04.

see Sur, Subramanian & Brandenburg (2007) for the corresponding case with magnetic fields. Finally, the neglect of the pressure term in the simple form of the  $\tau$  approximation is not justified, and a more rigorous treatment might alter the results significantly.

Next, we consider the case with a magnetic field and look at the dependence of  $\kappa_t$  and  $\kappa_{BB}$  on the magnetic field strength for fixed  $Pe = 1.8$ ; see Fig. 4. The function  $\kappa_B$  is also plotted, but, as expected, it is compatible with zero. Again,  $\kappa_t$  decreases with increasing field strength, but  $\kappa_{BB}$  is finite and positive, and increases with  $B_0$ .

The dependence of  $\kappa_t$  and  $\kappa_{BB}$  on  $Pe$  is shown in Fig. 5. Both functions increase with  $Pe$  as long as  $Pe$  is below about 10, and then seem to level off, although it would be desirable to confirm this for larger values of  $Pe$ . The  $Pe$  dependence of  $\kappa_t$  is similar to that for  $B_0 = 0$  and  $Co = 0.6$  where  $\kappa_t$  goes to zero with decreasing  $Pe$  like  $0.4 Pe$ , and  $\kappa_{BB} \approx 0.05 Pe^2$ , which is reminiscent of the behaviour of  $\kappa_\Omega$  for  $B_0 = 0$  and  $Co = 0.6$ .

Finally, we consider the dependence of the components of  $\kappa_{ij}$  on the wavenumber  $k$  of the test scalar in equations (16) and (17). A dependence of  $\kappa_{ij}$  on  $k$  reflects the fact that there is poor scale separation, i.e.  $k/k_f$  is not very small. In such a case (as already discussed in Section 2), the multiplication with a turbulent diffusivity in equation (3) must be replaced by a convolution with an integral kernel, as in Brandenburg, Rädler & Schinnerer (2008b) for the case of magnetic diffusion and  $\alpha$  effect. In Fourier space, the convolution

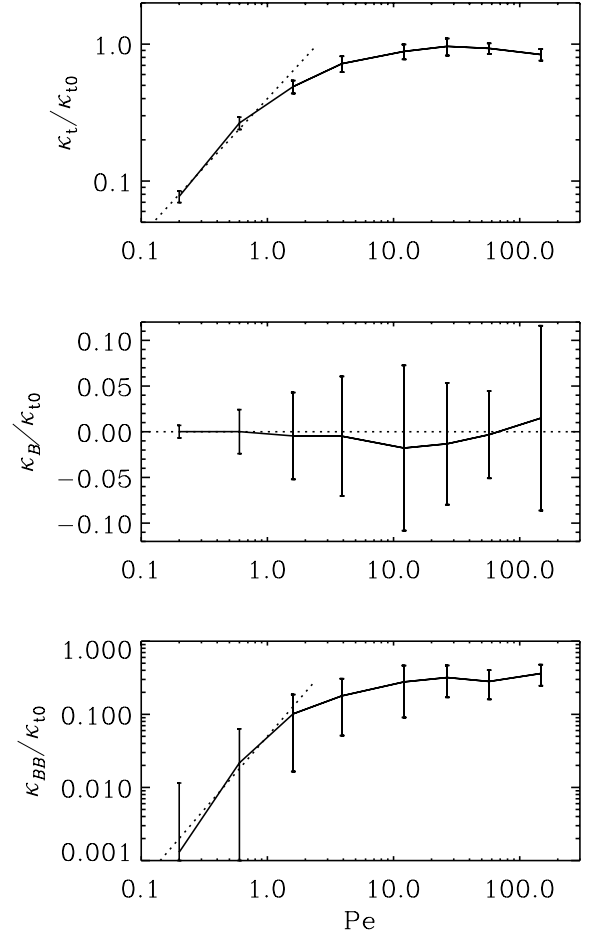


**Figure 5.**  $Pe$  dependence for  $Co = 0$  and  $B_0/B_{eq} = 1.3$ . The dotted lines in the first and last panel correspond to  $0.4 Pe$  and  $0.05 Pe^2$ , respectively. For the run with the largest value of  $Pe$ , we have  $\varepsilon = 0.20$ .

corresponds to a multiplication. As long as we consider monochromatic mean fields (proportional to  $e^{ik \cdot x}$  for a single wavevector), the values of the numerically determined components of  $\kappa_{ij}$  correspond to the value of the Fourier transform  $\tilde{\kappa}_{ij}$  at wavevector  $\mathbf{k}$ . The full integral kernel can then be assembled by determining the full  $\mathbf{k}$  dependence and then Fourier transforming back into real space.

In Fig. 6, we show the resulting dependences  $\tilde{\kappa}_t(k)$ ,  $\tilde{\kappa}_\Omega(k)$ , and  $\tilde{\kappa}_{\Omega\Omega}(k)$ , similar to earlier work on turbulent magnetic diffusion (Brandenburg et al. 2008b). It turns out that both  $\tilde{\kappa}_t$  and  $\tilde{\kappa}_\Omega$  can be fitted reasonably well to a Lorentzian,

$$\tilde{\kappa}_i = \frac{\tilde{\kappa}_{i0}}{1 + (ak/k_f)^2}, \quad (19)$$

where  $a \approx 0.62$ . This value of  $a$  is close to the corresponding value for turbulent magnetic diffusion where  $a \approx 0.5$  was found for the isotropic case (Brandenburg et al. 2008b) and  $a \approx 0.7$  in the anisotropic case with shear, but no rotation (Mitra et al. 2009). However, the coefficients  $\tilde{\kappa}_{t0}$  and  $\tilde{\kappa}_{\Omega0}$  depend on value of  $k_f/k_1$ . For  $k_f/k_1 = 3$ , we find  $\tilde{\kappa}_{t0}/\kappa_{t0} = 1.4$  and  $\tilde{\kappa}_{\Omega0} \approx 0.3$ , while for  $k_f/k_1 = 8$  we find  $\tilde{\kappa}_{t0}/\kappa_{t0} = 1.5$  and  $\tilde{\kappa}_{\Omega0}/\kappa_{t0} \approx 0.5$ . To make the curves for different values of  $k_f$  and  $Pe$  more nearly overlap, we have scaled  $\kappa_t$  by a factor  $s_t = k_f/k_1$ ,  $\kappa_\Omega$  by a factor  $s_\Omega = (k_f/k_1)^{1.7}$ , and  $\kappa_{\Omega\Omega}$  by a factor  $s_{\Omega\Omega} = (k_f/k_1)^{0.5}$ .

A surprising result occurs for  $\tilde{\kappa}_{\Omega\Omega}(k)$  which takes large negative values for  $k/k_f \approx 1$ , but tends to vanish for  $k \rightarrow 0$ . This means that the diffusion of mean fields along the axis of rotation is strongly

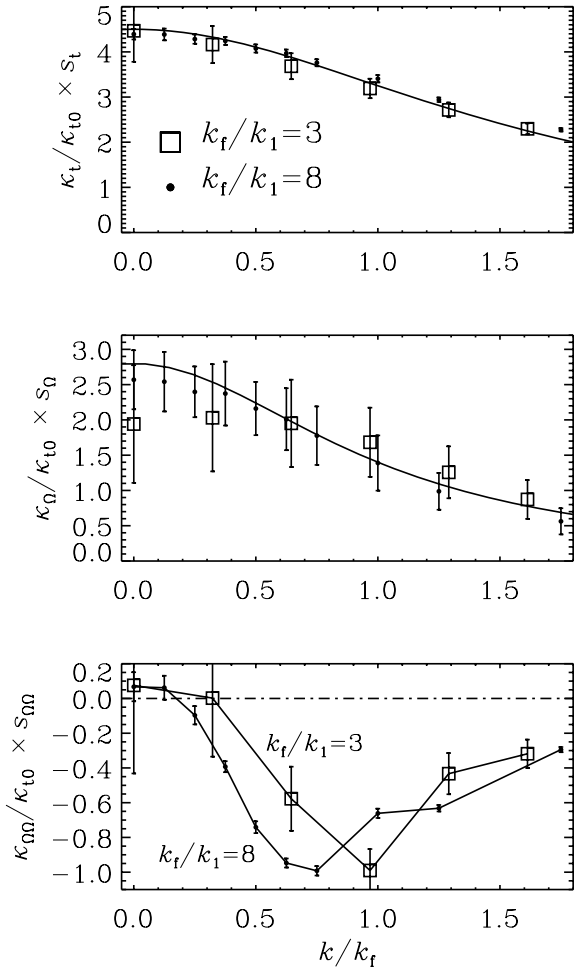


**Figure 6.** Wavenumber dependence of  $\kappa_t$ ,  $\kappa_\Omega$  and  $\kappa_{\Omega\Omega}$  for  $\text{Co} = 0.6$  and  $k_f/k_1 = 8$  with  $\text{Pe} = 70$  compared with the case  $k_f/k_1 = 3$  with  $\text{Pe} = 17$ . In the upper two panels, the lines represent curves of the form (19) with  $a = 0.62$  and  $0.5$ , respectively. For these runs, the anisotropy parameter  $\varepsilon$  is around  $0.003$  for the runs with  $k_f/k_1 = 8$  and  $\text{Pe} = 70$  and around  $0.036$  for the runs with  $k_f/k_1 = 3$  and  $\text{Pe} = 17$ .

suppressed once its typical length-scale becomes comparable with the scale of the energy-carrying eddies.

The two cases shown in Fig. 6 differ not only in the value of  $k_f/k_1$  (3 and 8), but also in the value of  $\text{Pe}$  (17 and 70). In order to show that the dependence of the scaling coefficients  $\tilde{\kappa}_{t0}$  and  $\tilde{\kappa}_{\Omega 0}$  is primarily due to the change in  $k_f/k_1$  we plot in Fig. 7 the dependence of  $\kappa_t$ ,  $\kappa_\Omega$  and  $\kappa_{\Omega\Omega}$  on the forcing wavenumber  $k_f/k_1$  for  $k = 0$  with  $\text{Co} = 0.6$  and  $\text{Pe} \approx 17$ . It turns out that both  $\kappa_t$  and  $\kappa_\Omega$  decrease with  $k_f$  like  $k_f^{-1}$ , while  $\kappa_{\Omega\Omega}$  is essentially compatible with zero.

In order to illustrate the meaning of the error bars, we show in Fig. 8 time series of  $\kappa_t$ ,  $\kappa_\Omega$  and  $\kappa_{\Omega\Omega}$  for a run in Fig. 6 with  $k = 0$ ,  $k_f/k_1 = 8$ ,  $\text{Co} = 0.6$ , and  $\text{Pe} = 70$ . Time is given in turnover times and covers nearly 200 in those units. This results in nearly 200 independent measurements, whose standard deviation yields the  $1\sigma$  probability range of finding measurements to lie in that interval.

In Fig. 9, we show the  $k$  dependence of the transport coefficients in the presence of a magnetic field and without rotation. The  $k$  dependence of  $\kappa_t$  is about that found in Fig. 6, but now  $\kappa_{\text{BB}}$  shows a marked dependence with a sign change at  $k/k_f \approx 0.5$  about values of  $\kappa_{\text{BB}}$  of opposite sign with extrema of similar modulus,

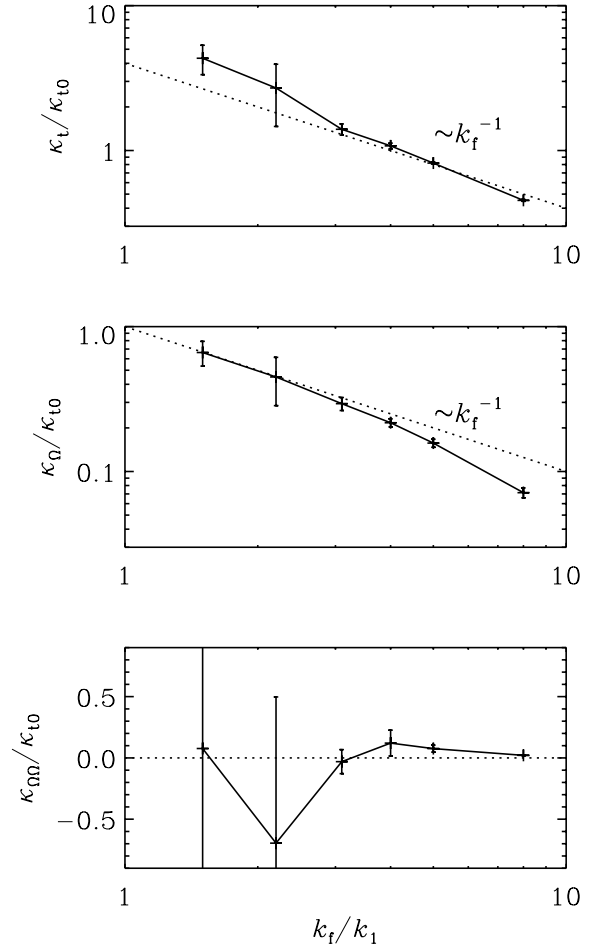


**Figure 7.** Dependence of  $\kappa_t$ ,  $\kappa_\Omega$  and  $\kappa_{\Omega\Omega}$  on the forcing wavenumber  $k_f/k_1$  for  $k = 0$  with  $\text{Co} = 0.6$  and  $\text{Pe} \approx 17$ . Note the scaling of  $\kappa_t$  and  $\kappa_\Omega$  with  $k_f^{-1}$ , while  $\kappa_{\Omega\Omega}$  is essentially compatible with zero.

$\kappa_{\text{BB}}/\kappa_{t0} \approx +0.3$  at  $k/k_f \approx 0$  and  $\kappa_{\text{BB}}/\kappa_{t0} \approx -0.3$  at  $k/k_f \approx 1$ . Furthermore, for  $k \rightarrow 0$  and  $k \rightarrow \infty$  the values of  $\kappa_{\text{BB}}$  are small.

## 5 CONCLUSIONS

The test scalar formalism described above proves to be a useful tool for calculating the components of the turbulent diffusion tensor for the mean passive scalar concentration. Here, the mean passive scalar concentration is defined as a two-dimensional field obtained by averaging over one coordinate direction. Therefore, the diffusion tensor has six relevant components. In the present investigation, we have only looked at the case of homogeneous turbulence where anisotropy is produced either by rotation or by a magnetic field. Another interesting alternative would be to look at the effects of a linear shear flows of the form  $\bar{\mathbf{U}}^S = (0, Sx, 0)$ . Investigations of the corresponding magnetic case with the test field method have already been carried out (Brandenburg et al. 2008a), and they confirmed the similarity between cases with shear and rotation. The application of the test scalar method to cases with shear would therefore be straightforward.

The test scalar method is analogous to the test field method for obtaining turbulent transport coefficients for the evolution of the mean magnetic field. Therefore, many of the questions raised in that case carry over to the present case. An example is the dependence of the transport coefficients on the length and time-scales of

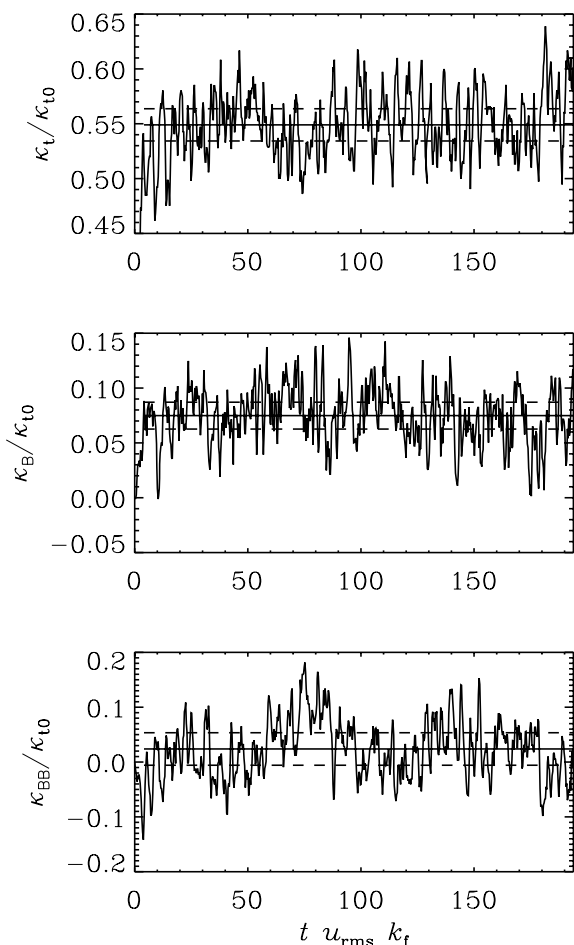


**Figure 8.** Time series of  $\kappa_t$ ,  $\kappa_\Omega$  and  $\kappa_{\Omega\Omega}$  for a run in Fig. 6 with  $k = 0$ ,  $k_f/k_1 = 8$ ,  $\text{Co} = 0.6$  and  $\text{Pe} = 70$ . The average values are shown as straight solid lines and the error margin is indicated by dashed lines.

the mean field. Usually, rapid spatial and temporal variations are less efficiently diffused by turbulence whose correlation length and time are no longer small compared with the corresponding scale of variation of the mean field.

A surprising result of the present work is the fact that turbulent transport along the rotation axis is not strongly reduced unless the length-scale of the mean field becomes comparable with the correlation length of the turbulence, i.e. when  $k \approx k_f$ . In that case, there is significant suppression of the turbulence along the direction of rotation. A similar result also applies if anisotropy is produced by an applied magnetic field.

The present investigation is restricted to the case when the scalar field is passive. This applies to the evolution of the entropy density in situations where an isothermal equation of state applies and where gravitational stratification is negligible. However, once gravitational stratification or non-isothermal effects become important, the test scalar formalism can only be used to describe small departures from a given reference state. It would be worthwhile exploring this case further.

Our work has shown that for non-helically forced isotropic turbulence, i.e. without rotation or magnetic fields, the turbulent diffusivity of a passive scalar is similar to the value of the turbulent diffusivity of the magnetic field in the kinematic limit. While this was expected based on results from the first-order smoothing approximation, the situation is less clear for turbulent kinematic

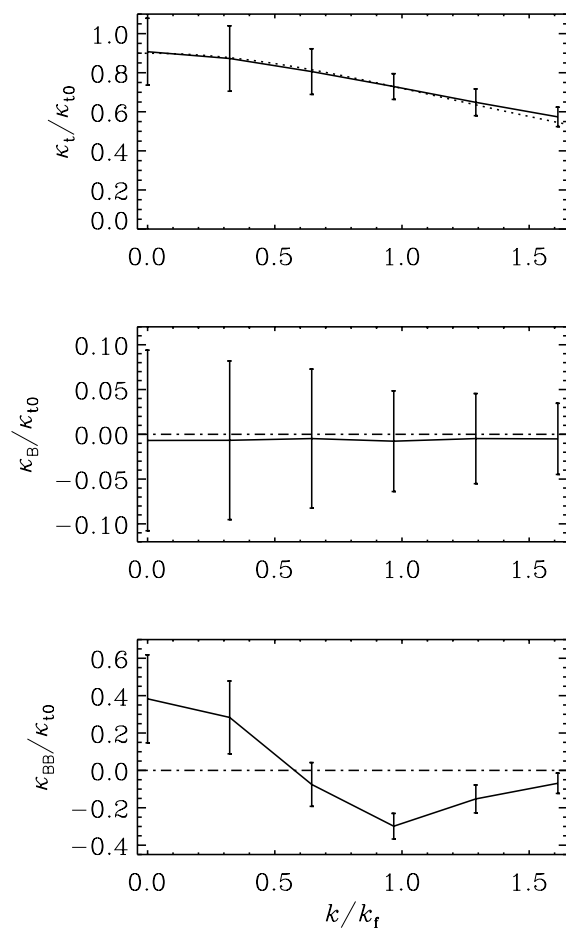


**Figure 9.** Wavenumber dependence of  $\kappa_t$ ,  $\kappa_B$  and  $\kappa_{BB}$  for  $\text{Co} = 0$ ,  $|\mathbf{B}|/B_{\text{eq}} = 1.4$  and  $\text{Pe} = 12$ . The dotted line represents a curve of the form (19) with  $a = 0.50$ . For these runs, the anisotropy parameter  $\varepsilon$  is around 0.13.

viscosity, which suggest that the turbulent magnetic Prandtl number should be  $2/5$ . Simulations of Yousef, Brandenburg & Rüdiger (2003), based on the decay rates of large-scale magnetic and velocity structures, have shown that the turbulent magnetic Prandtl number is indeed also unity. However, their method is not very accurate and it would be good to reconsider this by developing a method analogous to the test field and test scalar methods for test flows.

## ACKNOWLEDGMENTS

We thank Günther Rüdiger for detailed discussions regarding the sign of  $\kappa_\Omega$ , and for telling us about a sign error in the corresponding expression in Kitchatinov et al. (1994). The computations have been carried out at the National Supercomputer Centre in Linköping and at the Center for Parallel Computers at the Royal Institute of Technology in Sweden. This work was supported in part by the Swedish Research Council, grant 621-2007-4064 (AB) and the Sweden America Foundation through the Borgrättsfonderna, administered by the Office of Marshall of the Realm of Sweden (AS).

## REFERENCES

- Blackman E. G., Field G. B., 2003, *Phys. Fluids*, 15, L73  
 Brandenburg A., 2005, *Astron. Nachr.*, 326, 787

- Brandenburg A., Käpylä P., Mohammed A., 2004, *Phys. Fluids*, 16, 1020
- Brandenburg A., Rädler K.-H., Rheinhardt M., Käpylä P. J., 2008a, *ApJ*, 676, 740
- Brandenburg A., Rädler K.-H., Schrunner M., 2008b, *A&A*, 482, 739
- Durney B. R., Roxburgh I. W., 1971, *Solar Phys.*, 16, 320
- Gough D. O., 1978, in Belvedere G., Paternò L., eds, *Proc. EPS Workshop on Solar Rotation*. Catania Univ. Press, Catania, p. 337
- Haugen N. E. L., Brandenburg A., Dobler W., 2004, *Phys. Rev. E*, 70, 016308
- Hubbard A., Brandenburg A. 2008, *ApJ*, submitted (arXiv:0811.2561)
- Julien K., Legg S., McWilliams J., Werne J., 1996, *J. Fluid Mech.*, 322, 243
- Käpylä P. J., Korpi M. J., Tuominen I., 2004, *A&A*, 422, 793
- Kitchatinov L. L., Rüdiger G., 1995, *A&A*, 299, 446
- Kitchatinov L. L., Mazur M. V., 2000, *Solar Phys.*, 191, 325
- Kitchatinov L. L., Rüdiger G., Pipin V. V., 1994, *Astron. Nachr.*, 315, 157
- Kleeorin N. I., Rogachevskii I. V., Ruzmaikin A. A., 1990, *Sov. Phys. JETP*, 70, 878
- Mitra D., Käpylä P. J., Tavakol R., Brandenburg A., 2009, *A&A*, 495, 1
- Rieutord M., Brandenburg A., Mangeney A., Drossart P., 1994, *A&A*, 286, 471
- Rüdiger G., 1989, *Differential Rotation and Stellar Convection: Sun and Solar-Type Stars*. Gordon & Breach, New York
- Rüdiger G., Pipin V. V., 2001, *A&A*, 375, 149
- Rüdiger G., Hollerbach R., 2004, *The Magnetic Universe*. Wiley-VCH, Weinheim
- Rüdiger G., Egorov P., Kitchatinov L. L., Küker M., 2005, *A&A*, 431, 345
- Schrinner M., Rädler K.-H., Schmitt D., Rheinhardt M., Christensen U., 2005, *Astron. Nachr.*, 326, 245
- Schrinner M., Rädler K.-H., Schmitt D., Rheinhardt M., Christensen U. R., 2007, *Geophys. Astrophys. Fluid Dyn.*, 101, 81
- Sur S., Subramanian K., Brandenburg A., 2007, *MNRAS*, 376, 1238
- Sur S., Brandenburg A., Subramanian K., 2008, *MNRAS*, 385, L15
- Thompson M. J., Christensen-Dalsgaard J., Miesch M. S., Toomre J., 2003, *ARA&A*, 41, 599
- Vainshtein S. I., Kitchatinov L. L., 1983, *Geophys. Astrophys. Fluid Dyn.*, 24, 273
- Vitense E., 1953, *Z. Astrophys.*, 32, 135
- Weiss N. O., 1965, *Observatory*, 85, 37
- Yousef T. A., Brandenburg A., Rüdiger G., 2003, *A&A*, 411, 321

## APPENDIX A: THE POSITIVE SIGN OF $\kappa_\Omega$

In this appendix, we motivate the origin of the positive sign of  $\kappa_\Omega$  using the pressureless  $\tau$  approximation. In this approach, one considers the evolution equation for  $\overline{\mathcal{F}}$ ,

$$\frac{\partial \overline{\mathcal{F}}_i}{\partial t} = \overline{u_i \dot{c}} + \overline{u_i \dot{c}}, \quad (\text{A1})$$

where dots denote time derivatives (Blackman & Field 2003; Brandenburg, Käpylä & Mohammed 2004). We use equations (10)

and (12), assume that  $\mathbf{u} = \mathbf{U}$ , i.e. that  $\overline{\mathbf{U}} = 0$ , ignore the pressure term and magnetic fields, assume  $\overline{f^c} = 0$ , and obtain

$$\overline{u_i \dot{c}} = -2\Omega_j \epsilon_{ijk} \overline{u_k \dot{c}} + \text{triple correlations}, \quad (\text{A2})$$

$$\overline{u_i \dot{c}} = -\overline{u_i u_j} \nabla_j \overline{c} + \text{triple correlations}. \quad (\text{A3})$$

The triple correlation terms result from the non-linearities in the evolution equations (10) and (12). In the  $\tau$  approximation, we substitute the sum of the triple correlations by quadratic correlations, i.e. by  $-\overline{u_i \dot{c}}/\tau$  in the present case (Vainshtein & Kitchatinov 1983; Kleeorin, Rogachevskii & Ruzmaikin 1990). We write the resulting equation in matrix form,

$$\tau \frac{\partial \overline{\mathcal{F}}_i}{\partial t} = -\mathbf{L}_{ik} \overline{\mathcal{F}}_k - \tau \overline{u_i u_j} \nabla_j \overline{c}, \quad (\text{A4})$$

where  $\mathbf{L}_{ik} = \delta_{ik} + 2\Omega_j \tau \epsilon_{ijk}$ . We solve this equation for  $\overline{\mathcal{F}}$  and obtain

$$\overline{\mathcal{F}}_i = -(\mathbf{L}^{-1})_{ij} \left( \tau \overline{u_j u_k} \nabla_k \overline{c} + \tau \frac{\partial \overline{\mathcal{F}}_i}{\partial t} \right), \quad (\text{A5})$$

where

$$\mathbf{L}^{-1} = \frac{1}{1 + \text{Co}^2} \begin{pmatrix} 1 & \text{Co} & 0 \\ -\text{Co} & 1 & 0 \\ 0 & 0 & 1 + \text{Co}^2 \end{pmatrix} \quad (\text{A6})$$

and

$$\overline{u_j u_k} = \text{diag} \left( \overline{u_\perp^2}, \overline{u_\perp^2}, \overline{u_\parallel^2} \right). \quad (\text{A7})$$

In the stationary state, we may ignore the time derivative and recover equations (3) and (4) with

$$\kappa_t = \frac{\tau \overline{u_\perp^2}}{1 + \text{Co}^2}, \quad \frac{\kappa_\Omega}{\kappa_t} = \text{Co}, \quad \frac{\kappa_{\Omega\Omega}}{\kappa_t} = \frac{\text{Co}^2 + \varepsilon}{1 - \varepsilon}, \quad (\text{A8})$$

where  $\varepsilon = 1 - \overline{u_\perp^2}/\overline{u_\parallel^2}$  was defined in equation (8). In the cases reported here, the value of  $\varepsilon$  was never found to be negative. Note also that  $1 - \varepsilon = \overline{u_\perp^2}/\overline{u_\parallel^2}$  in the denominator of equation (A8) is always positive. Therefore, in addition to  $\kappa_\Omega$  being positive, also  $\kappa_{\Omega\Omega}$  should be positive.

This paper has been typeset from a  $\text{\TeX}/\text{\LaTeX}$  file prepared by the author.